Astron. Astrophys. 203, 348–354 (1988)

ASTRONOMY AND ASTROPHYSICS

51 Ophiuchi (B9.5 Ve): A Be star in the class of β Pictoris stars?*

L.B.F.M. Waters[1], J. Coté[1], and T.R. Geballe[2,]**

[1] Astronomical Institute, University of Amsterdam, Roetersstraat 15, 1018 WB Amsterdam, The Netherlands
[2] United Kingdom Infrared Telescope, 665 Komohana Street, Hilo, Hawaii 96720, USA

Received July 27, 1987; accepted January 26, 1988

Summary. The UV to far-IR energy distribution of the B9.5 Ve star 51 Oph is presented. This star shows a normal UV and visual continuum energy distribution, but a large IR excess caused by circumstellar dust with temperatures between about 1000 and 130 K. 51 Oph is the only Be star of a sample of 101 that shows an IR excess due to circumstellar dust. The far-IR energy distribution of 51 Oph is very peculiar when compared to those of Be, Ae and A-shell stars. A simple optically thin dust model is used to fit the observed IR excess. It is found that the density of the dust particles decreases as $n(r) \propto r^{-m}$, with $m \simeq 1.3$, and the absorption coefficient of the dust $Q(\nu) \propto \nu^{p}$, with p between 1 and 2. The dust around 51 Oph is in many aspects similar to that of β Pic. The relation between 51 Oph and the class of β Pic stars is discussed.

Key words: stars: Be – stars: circumstellar dust

1. Introduction

IRAS observations of the Be star 51 Oph (B9.5 Ve) revealed a very strange energy distribution in the far-IR (Coté and Waters, 1987, hereafter referred to as Paper I). The star showed a very large IR excess at 12 μ of $3^{m}.6$, which is much larger than the excess of $0^{m}.5$ to $1^{m}.0$ usually found for B8–B9 emission line stars (Paper I). This large IR excess is due to circumstellar dust. 51 Oph is the only Be star out of a sample of 101 studied in Paper I that shows clear evidence for circumstellar dust. Furthermore, the far-IR colours strongly deviate from those typical for Be stars. In fact, no other hot star observed with IRAS shows far-IR colours similar to those of 51 Oph.

Almost all Be stars show an excess of IR emission when compared to "normal" stars. This excess emission is interpreted as due to free-free radiation from an ionized high-density envelope around the star, which is also responsible for the Hα emission (e.g., Poeckert and Marlborough, 1978). In Paper I it was shown that the observed far-IR energy distribution of Be stars is well represented by a power-law of the shape $S_{\nu} \propto \nu^{\alpha}$ with α between 0.6 and 2. The observed energy distribution is explained by assuming a disc with a power-law density distribution of the type $\rho(r) \propto r^{-n}$, with n between 2 and 3.5 (Waters et al., 1987).

In this paper, we study the peculiar energy distribution of 51 Oph (=HD 158643 =HR 6519). In Sect. 2, we discuss the observed UV to far-IR energy distribution of 51 Oph. In Sect. 3, we compare this energy distribution with those of Be, Ae and A-shell stars, and in Sect. 4 we present a simple optically thin dust emission model. In Sect. 5 we apply this model to the observed excess in 51 Oph. In Sect. 6 we discuss the nature of 51 Oph and the relation between this star and the class of β Pic stars.

2. The energy distribution

The observed energy distribution of 51 Oph is plotted in Fig. 1. The UV observations were taken from the S2/68 photometric catalogue (Thompson et al., 1978). Visual photometry was taken from Johnson et al. (1966). Near-IR observations were obtained with the UKIRT telescope at Hawaii. IRAS photometry was taken from the IRAS Point Source Catalogue (Explanatory Supplement, 1985, hereafter referred to as IRAS PSC), and was colour-corrected. We corrected for interstellar extinction using the Savage and Mathis (1979) extinction curve and $E(B-V) = 0.04$, which resulted from the intrinsic $(B-V)_0$ colour for a B9.5 V star given by FitzGerald (1970) and the observed value of $(B-V) = 0.00$. The observed magnitudes and absolute fluxes are listed in Table 1.

We have compared the UV and visual energy distribution of 51 Oph with the grid of model atmospheres published by Kurucz (1979), and found a "best fit" for the model with parameters $T_{\rm eff} = 9500$ K and $\log g = 4.0$, i.e. typical values for a B9.5 V star. We show the Kurucz model in Fig. 1 (solid line).

It is clear from Fig. 1 that 51 Oph has a large IR excess for wavelengths longwards of 2.2 μ. The IR excess is not typical for Be stars, but clearly indicates the presence of circumstellar dust. The excess of $3^{m}.6$ at 12 μ is much larger than found in other late B-type Be stars (typically $0^{m}.5$ to $1^{m}.0$, Paper I). This is the only Be star in the sample of 101 stars discussed in Paper I that shows clear evidence for circumstellar dust. This property is probably closely related to its spectral type, very close to A0. The Ae stars

Send offprint requests to: L.B.F.M. Waters

* Partly based on IRAS observations. The Infrared Astronomical Satellite was developed and operated by the Netherlands Agency for Aerospace Programs, the U.S National Aeronautic and Space Administration, and the U.K. Science Engineering and Research Council.

** Affiliated with the Foundation for Astronomical Research in the Netherlands (ASTRON)

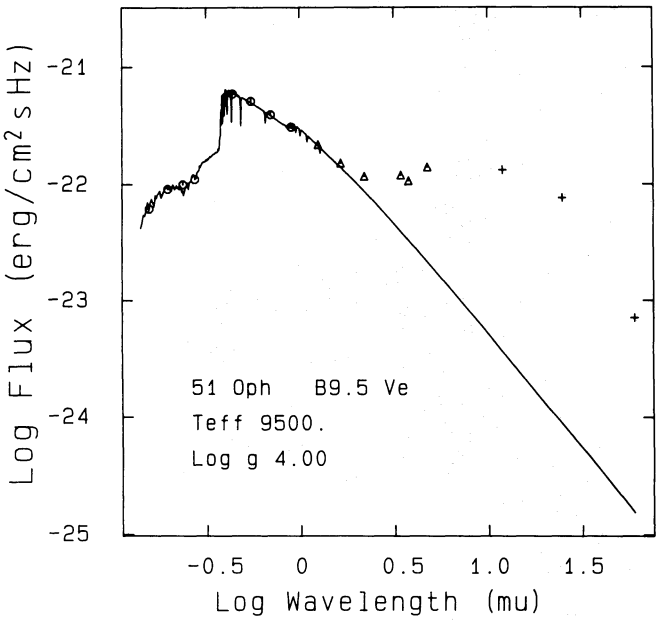

Fig. 1. The observed dereddened energy distribution of 51 Oph. Circles are UV and visual photometry (Thompson et al., 1978; Johnson et al., 1966), triangles are near-IR observations (this paper, Table 1), and plusses are IRAS data. The solid line is the "best fit" Kurucz model (1979) model atmosphere based on the UV and visual fluxes

Table 1. The observed magnitudes and absolute fluxes

$\lambda(\mu)$	m_λ mag	$\log F_\nu$ (erg cm^{-2} s^{-1} Hz^{-1})[a]
0.1565		−22.210
0.1965		−22.042
0.2365		−22.003
0.2740		−21.229
0.44	4.81	−21.229
0.55	4.81	−21.291
0.70	4.74	−21.406
0.90	4.72	−21.512
1.25	4.61[b]	−21.662
1.65	4.53[b]	−21.821
2.20	4.31[b]	−21.932
3.45	3.46[b]	−21.922
3.80	3.38[b]	−21.972
4.80	2.60[b]	−21.855
12	1.04	−21.879[c]
25	−0.08	−22.117[c]
60	0.44	−23.149[c]

[a] The absolute fluxes are extinction corrected.
[b] The UKIRT observations were obtained on May 23, 1986. The errors in the observed magnitudes are of the order of 0^m.01.
[c] The IRAS fluxes were corrected for bandwidth effects.

Table 2. The excess fluxes

$\lambda(\mu)$	$\log F$(excess) (erg cm^{-2} s^{-1} Hz^{-1})
2.2	−22.525
3.45	−22.097
3.80	−22.134
4.80	−21.928
12.	−21.891
25.	−22.122
60.	−23.157

tend to show excess IR emission due to circumstellar dust rather than due to free-free emission from ionized gas.

The presence of Hα emission clearly indicates that ionized material is present around this star. This material can also contribute to the IR excess through free-free emission. However, the contribution of the thermal dust emission to the total flux is likely to be much larger than that of free-free emission. In the near-IR, the shape of the excess flux energy distribution (listed in Table 2 and plotted in Fig. 7) cannot be explained by free-free emission, since the energy distribution of ionized gas emitting free-free and free-bound radiation $F_\nu \propto \nu^\alpha$, with $0 \leq \alpha \leq 2$ (e.g. Wright and Barlow, 1975). In 51 Oph the slope of the excess flux energy distribution between 2.2 and 4.8 μ is $\alpha \simeq -1.7$, i.e. incompatible with the slope expected for free-free emission. Furthermore, the size of the excess is much larger than for other late B-type Be stars. These stars usually have excesses in the wavelength range between 2 and 5 μ of the order of 0.1 to 0.2 μ or even no excess at all (e.g. Gehrz et al., 1974; Dachs and Wamsteker, 1982; Ashok et al., 1984). Similar arguments hold for the IRAS wavelength region. For instance, the B9.5 Ve star κ^1 Lup has an excess of only 0^m.29 at 12 μ (Paper I). Furthermore, the shape of the 12 to 60 μ energy distribution is not typical for free-free emission. We conclude that the contribution of free-free emission to the IR excess in 51 Oph is negligible.

3. Comparison with Ae and A-shell stars

The facts that 51 Oph has a circumstellar dust cloud, and that its spectral type is close to A0, suggest that it may be more closely related to the Ae and A-shell stars than the Be stars. In order to investigate this further, we have compared the far-IR properties of 51 Oph with those of known Ae and A-shell stars detected with IRAS. Jaschek et al. (1986) have published a list with Ae and A-shell stars detected with IRAS.

In Fig. 2 we have plotted the IRAS far-IR colour-colour diagram for the Ae and A-shell stars listed by Jaschek et al. (1986). The fluxes are taken from the IRAS PSC. We have also included the observed colours of 51 Oph. We indicate the position of blackbodies (solid line) and of power-law energy distributions (dashed line) in Fig. 2. The position of the Be stars (Paper 1) is indicated by the rectangle.

Figure 2 shows that the far-IR energy distribution of most of the Ae and A-shell stars can be represented by a power-law of the shape $S_\nu \propto \nu^\alpha$, with α between 0 and −1.5. This strongly suggests that the excess is due to thermal dust emission, since the value of α expected from free-free emission cannot be smaller than zero

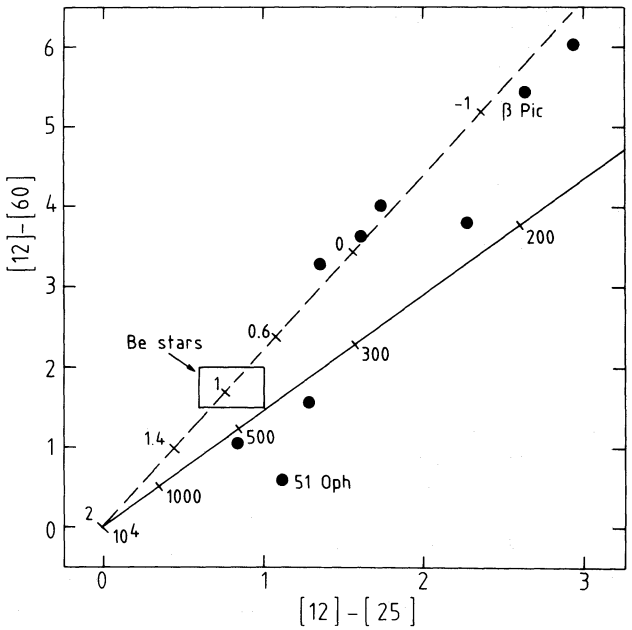

Fig. 2. IRAS far-IR colour-colour diagram of Ae and A-shell stars. The solid line represents the position of blackbodies with different temperatures, and the dashed line the position of power-law energy distributions of the shape $S_\nu \propto \nu^\alpha$. The numbers indicate some values for the temperature and α. The box indicates the position of the classical Be stars (Paper I). Notice that most of the Ae stars lie close to the power-law line, and that 51 Oph shows a deviating behaviour

(Wright and Barlow, 1975), i.e. the case for optically thin emission. The value of α found for the Be stars lies in the range 0.6 to 2 (Waters et al., 1987). The fact that the far-IR energy distribution of Ae and A-shell stars is a power-law rather than a blackbody (at least at wavelengths between 12 and 60 μ) suggests that the dust particles have a range of temperatures. In the next Section we will show that the shape of the spectrum can be used to derive the density distribution of the dust particles if they are in thermal equilibrium.

The position of 51 Oph in Fig. 2 strongly deviates from that of the Ae and A-shell stars, since it lies neither on the blackbody line, nor on the power-law line. In fact, the 25 to 60 μ slope of the energy distribution suggests a value of $\alpha \simeq 2.7 > 2$, *i.e. steeper than the Rayleigh-Jeans tail of a blackbody*. Since this is very unusual in the wavelength range under consideration, we checked the quality of the 60 μ detection. The S/N ratio given in the IRAS PSC is 5. It is known that the flux of weak point sources can be overestimated (Explanatory Supplement, 1985). If the true 60 μ flux of 51 Oph would be lower than given in the IRAS PSC, the 25 to 60 μ slope would even be steeper. We also inspected the detector response as a function of time at 12 to 60 μ. There is some evidence for extended emission at the position of 51 Oph at 60 μ, but the point source is clearly present at the expected position. We conclude that the energy distribution of 51 Oph between 25 and 60 μ is steeper than that of a blackbody spectrum.

4. Optically thin dust emission

In this section, we discuss the emission from optically thin dust. We assume that the dust is in thermal equilibrium with the stellar radiation field, and that the radius of the dust particles a is constant. This assumption seems reasonable since Mezger et al. (1982) showed that the energy distribution of dust grains with a size distribution can be represented by the energy distribution of dust grains with an average size and an average temperature.

The flux observed at Earth from a (spherically symmetric) dust cloud around a star that extends from inner radius r_0 to outer radius r_1, and with a number density distribution $n_d(r) = n_0(r/R_*)^{-m}$, and an emission efficiency of the dust grains $Q(\nu) = Q_0(\nu/\nu_0)^p$, is:

$$F_\nu = \pi a^2 Q(\nu) n_0 4\pi D^{-2} R_*^m \int_{r_0}^{r_1} B_\nu(T(r)) r^{2-m}\, dr \tag{1}$$

(Sopka et al., 1985), where B_ν is the Planck function, and D is the distance of the star in cm. Thermal equilibrium gives:

$$T(r) = T_0(r/R_*)^{-2/(4+p)} \tag{2}$$

where T_0 is some normalization temperature (Sopka et al., 1985). In the case of gray particles ($p = 0$), this gives the familiar result $T(r) \propto r^{-1/2}$. Substituting Eq. (2) into Eq. (1) and changing the integral variable from r to $x = r/R_*$, where R_* is the stellar radius in cm, this gives:

$$F_\nu = 8\pi^2 a^2 n_0 R_*^3 D^{-2} h c^{-2} Q(\nu) \nu^3 \times \int_{x_0}^{x_1} x^{2-m} [\exp\{h\nu x^\beta / kT_0\} - 1]^{-1}\, dx \tag{3}$$

with $\beta = 2/(4 + p)$.

In order to show the frequency-dependency of Eq. (3) more clearly, it is convenient to change the integral variant from x to $y = (h\nu/kT_0)x^\beta$, yielding:

$$F_\nu = 8\pi^2 a^2 h c^{-2} n_0 R_*^3 D^{-2} Q(\nu) \nu^3 \left[\frac{kT_0}{h\nu}\right]^{(3-m)/\beta} \beta^{-1} G(y_0, y_1, m, \beta) \tag{4}$$

where $G(y_0, y_1, m, \beta)$ is defined as:

$$G(y_0, y_1, m, \beta) = \int_{y_0}^{y_1} y^{(3-m-\beta)/\beta} [\exp(y) - 1]^{-1}\, dy \tag{5}$$

In this expression y_0 and y_1 are the values of $(h\nu/kT_0)x^\beta$ at the inner and outer radius of the dust shell. The function $G(y_0, y_1, m, \beta)$ can be solved analytically for some cases. Assume y_0 and $y_1 \ll 1$, i.e. corresponding to high T_0 or low frequency, this gives:

$$F_\nu \propto \nu^{2+p} \tag{6}$$

So Eq. (6) gives the slope of the energy distribution in the long-wavelength limit.

Another interesting case occurs for $y_0 = 0$ and $y_1 =$ "∞", i.e. the long-wavelength spectrum of a dust cloud that extends from the surface of the star to infinity. In that case $G(y_0, y_1, m, \beta)$ does not depend on frequency, and we find

$$F_\nu \propto \nu^{3+p-0.5(3-m)(4+p)} \tag{7}$$

In general, the energy distribution of a dust cloud will show a slope as given by Eq. (7), with a turnover at high frequency due to the inner (hottest dust) radius of the dust, and a similar turnover due to the outer (coolest dust) radius of the dust shell. The positions of these "hot" and "cool" dust turnover frequencies can be estimated using Wiens displacement law. We find:

$$\nu_0 \simeq (3 + p)kT_d(x_0)/h \tag{8a}$$

$$\nu_1 \simeq 2(3 + p)kT_d(x_1)/h \tag{8b}$$

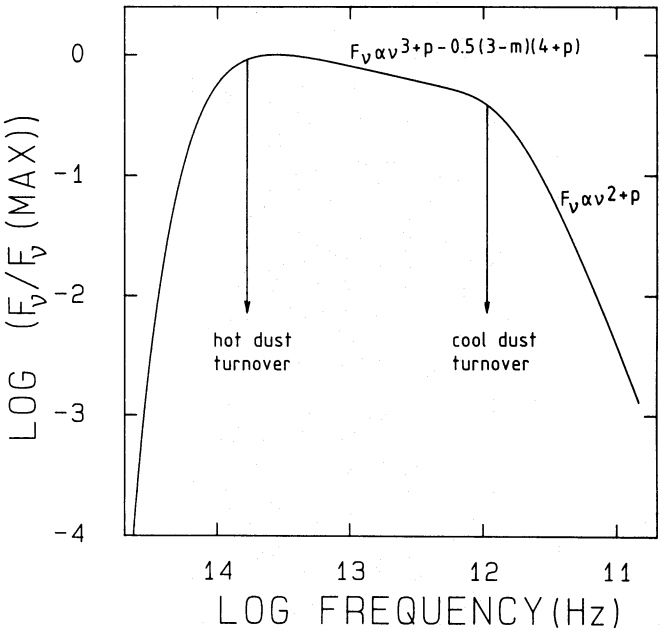

Fig. 3. A schematic plot of a typical energy distribution of dust grains in thermal equilibrium with the stellar radiation field. Indicated are the hot and cool dust turnover frequencies, and the slope of the spectrum between these frequencies and in the low frequency limit

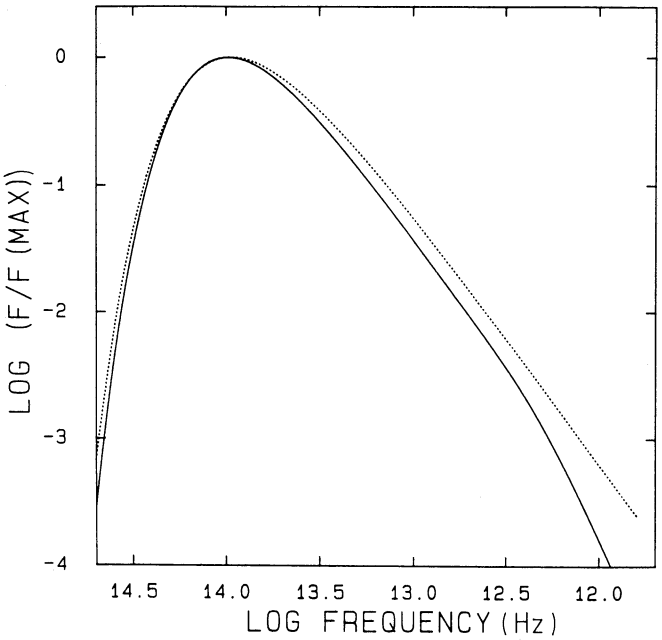

Fig. 5. The solid line is the resulting energy distribution of a dust shell with parameters $T_0 = 5000\,K$, $p = 2$, $m = 2$, $x_0 = 50$ and $x_1 = 10^7$. The dotted line is a single blackbody with a temperature of 1600 K. Notice the strong resemblance between both curves

The factor 2 in Eq. (8b) is due to the fact that the cool dust turnover is not a sharp bend in the energy distribution. In Fig. 3, we schematically show the resulting energy distribution of an optically thin dust shell. The hot and cool dust turnover frequencies are indicated.

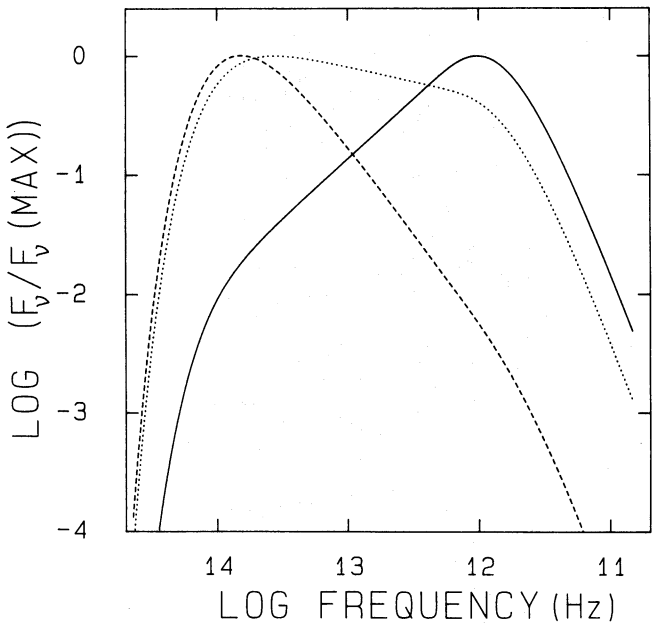

Fig. 4. The effect of different density distributions of the dust on the resulting energy distribution. A model with $T_0 = 5000$ K, $x_0 = 30$, $x_1 = 10^7$, $p = 1$ and $m = 1$ (solid line), $m = 1.5$ (dotted line), and $m = 2$ (dashed line) is used. Notice the sensitivity of the shape of the energy distribution on the parameter m

In Fig. 4 we show the effect of the density distribution of the dust on the resulting energy distribution. We adopted a model with parameters $T_0 = 5000$ K, $p = 1$, $x_0 = 30\,R_*$ and $x_1 = 1\,10^7\,R_*$, and $m = 1$, 1.5 and 2. Figure 4 illustrates the sensitivity of the energy distribution on the value of m. Especially the slope of the energy distribution between the hot and cool dust turnover frequencies changes drastically with m, in agreement with Eq. (7).

The energy distribution of optically thin dust with a temperature distribution can in some cases closely resemble that of a single blackbody. This is illustrated in Fig. 5 where we have plotted the resulting energy distribution for a dust model with parameters $p = 2$, $m = 2$, $T_0 = 5000$ K and $x_0 = 30\,R_*$ and $x_1 = 10^7\,R_*$. This spectrum shows a peak at a frequency of 10^{14} Hz. For comparison, we plotted the blackbody energy distribution with a temperature of 1600 K, corresponding to a maximum at 10^{14} Hz. The shape of both curves is remarkably similar.

In summary, the continuum energy distribution of dust in thermal equilibrium with the stellar radiation field will show a slope $\alpha = (3 + p) - 0.5(3 - m)(4 + p)$ between frequency ν_0 and ν_1, and a slope $\alpha = p + 2$ for $\nu \ll \nu_1$. In the next section, we will use this simple model to interpret the IR excess of 51 Oph.

5. Properties of the dust around 51 Oph

In this section, we apply the simple optically thin dust model to the IR excess observed in 51 Oph, in order to derive estimates of the parameters $p, m, T_d(x_0)$ and $T_d(x_1)$.

5.1. *Estimate of the value of p*

Equation (6) shows that for $\nu < \nu_1$ the slope of the energy distribution $s_\nu \propto \nu^\alpha$, with $\alpha = 2 + p$. From Table 1 we derive a value

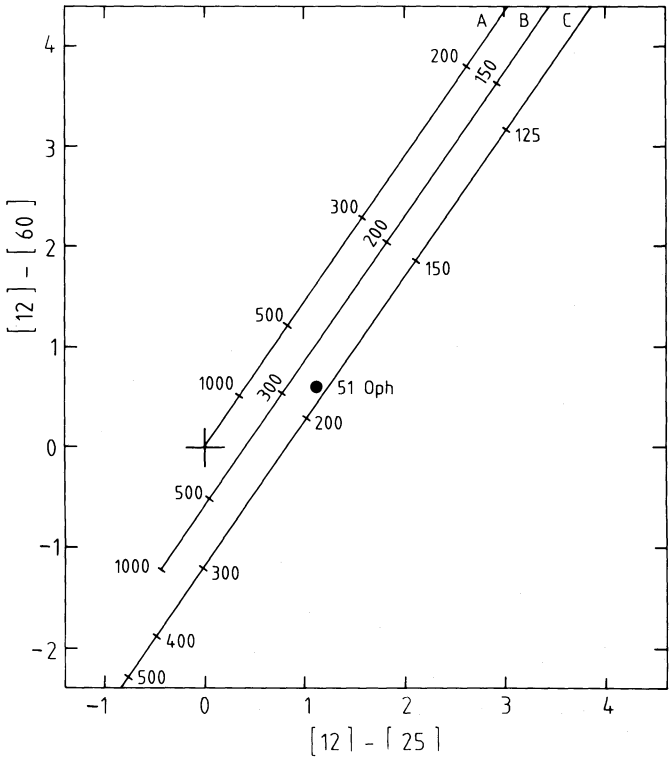

Fig. 6. The position of 51 Oph in the [12]–[25] versus [12]–[60] diagram is compared with that of dust grains radiating with an emission efficiency $Q(\nu) \propto \nu^p$ with $p = 0$ (case A) i.e. a single blackbody, $p = 1$ (case B) and $p = 2$ (case C). Some dust temperatures are indicated

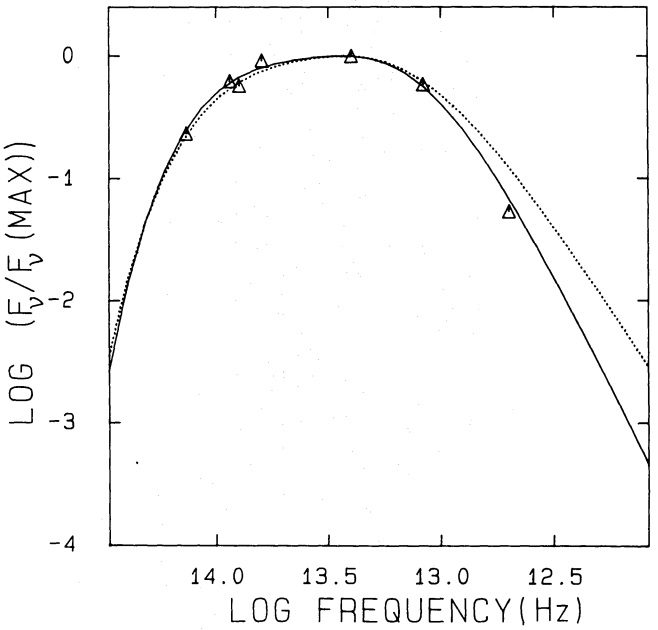

Fig. 7. The observed excess flux energy distribution (Table 2) is plotted versus frequency (triangles). We normalized the flux to the flux at 12 μ. The solid line is the resulting energy distribution of a dust model with parameters $p = 2$, m = 1.3, $T_0 = 7850$ K, $x_0 = 380$ and $x_1 = 2.7\,10^5$. The dashed line is the same for a model with parameters $p = 1$, $m = 1.36$, $T_0 = 7370$ K, $x_0 = 80$ and $x_1 = 16800$. Notice that the latter model fails to explain the 60 μ observation

for α between 25 and 60 μ of $\alpha = 2.7$, which would imply $p = 0.7$. However, the energy distribution may not have reached the low-frequency limit yet, so $p > 0.7$. In Fig. 6, we have plotted the location of optically thin dust radiating with $S_\nu \propto \nu^{p+2}$ in the IRAS [12]–[25] versus [25]–[60] diagram, for various dust temperatures. Figure 6 shows that this type of emissivity, with $p \simeq 1.5$ to 2, can explain the observed far-IR colours of 51 Oph. The dust temperature that is found is about 200 to 300 K. Notice that this temperature is far too low to explain the *near-IR* excess (Fig. 1). This requires temperatures of the order of 1000 K. So a range of temperatures is needed to explain the IR excess of 51 Oph. The value of p may not be constant over the whole wavelength range $1 < \lambda < 60\,\mu$. Jones and Merrill (1976) use $Q(\nu) \propto \nu^1$ for $\lambda < 50\,\mu$ and $Q(\nu) \propto \nu^2$ for $\lambda > 50\,\mu$. So a smaller value of p for shorter wavelengths cannot be excluded.

5.2. *The density distribution of the dust grains*

The slope of the energy distribution between the hot and cool dust turnover frequencies can be used to derive the density distribution of the dust, i.e. the parameter m. The dust contribution to the total flux can be derived using the Kurucz (1979) model to estimate the stellar photospheric fluxes. In Table 2, we list the excess fluxes, and they are plotted in Fig. 7. It is difficult to estimate the positions of the hot and cool turnover frequencies from Table 2. For $3.45 < \lambda < 12\,\mu$ the spectrum of the excess flux has a slope $\alpha = -0.4$, while for $4.8 < \lambda < 12\,\mu$ we find $\alpha = -0.09$. Rewriting Eq. (7) gives

$$m = \frac{6 + p + 2\alpha}{4 + p} \tag{9}$$

for $\alpha = -0.4$ and $p = 1.5$ (2.0) we find $m = 1.22$ (1.20). Similarly, if $\alpha = -0.09$, and $p = 1.5$ (2.0) we find $m = 1.33$ (1.30). We conclude that the value of m lies in the range $1.2 < m < 1.33$. Notice that even in the case of gray particles, i.e. $p = 0$, and $\alpha = -0.09$ we find $m < 2$.

In passing we note that the Ae and A-shell stars plotted in Fig. 2 have a spectral index α between 0 and about -1. For $p = 1$ this would imply values of m between 1.4 and 1, which is in the same range as found for 51 Oph.

5.3. *Estimates of the dust temperatures and inner and outer radius*

Having derived estimates of p and m, we can proceed in estimating the range in temperatures from the estimate of the turnover frequencies ν_0 and ν_1. Inspection of Fig. 7 and Table 2 shows that $\nu_0 \simeq 10^{14}$ Hz and $\nu_1 \simeq 2.5\,10^{13}$ Hz are reasonable estimates. These correspond to $T_d(x_0) = 1070$ K and $T_d(x_1) = 133$ K if $p = 1.5$, and to $T_d(x_0) = 960$ K and $T_d(x_1) = 120$ K if $p = 2$. Since we assumed that the dust particles are in thermal equilibrium (Eq. (3)), the range in temperatures can readily be converted to an inner and outer radius of the dust shell if an estimate of T_0

can be made. Sopka et al. (1985) give a simple method (based on the assumption of thermal equilibrium) to calculate T_0:

$$T_0 = T(x=1) = 4.802\,10^{-11}[5.397\,10^{45}\{(p+3)!\}^{-1}\int_0^\infty F_\nu^* \nu^p\,d\nu]^{1/4+p} \quad (10)$$

We have evaluated the integral in Eq. (10) using the Kurucz (1979) model atmosphere with $T_{\rm eff} = 9500$ K and $\log g = 4.0$ (Fig. 1), for p between 1 and 2, yielding $T_0 = 7370$ K and 7850 K for $p = 1$ and $p = 2$ respectively. So T_0 is not very sensitive to the value of p. We point out that the value of T_0 given above merely is a normalisation temperature, and does not imply that dust with such unrealistically high temperatures is present.

In the previous subsections we argued that there is still some freedom in the choice of the parameter p. The resulting values of the inner and outer radius of the dust shell depend strongly on p. The slope of the far-IR energy distribution (Fig. 6) indicates $p \simeq 1.5$ to 2. Therefore we fitted the observed excess fluxes with a dust model with parameters $p = 2$, $m = 1.3$, and $T_0 = 7850$ K. A 'best fit' was found for $x_0 = 380$ and $x_1 = 2.7\,10^5$, and is shown in Fig. 7 (solid line). Adopting $R_* \simeq 2\,R_\odot$, the size of the outer radius is 16600 AU, and with a distance of about 70 pc this corresponds to about 4 arcmin. This seems unrealistically large. For instance, the dust in β Pic extends to a distance of 400 AU (Gillett, 1986).

The outer radius of the dust shell can be smaller if the value of p is smaller. Therefore, we also tried some model fits with $p = 1$, and found a good fit for $T_0 = 7370$ K, $m = 1.36$, $x_0 = 80$ and $x_1 = 16{,}800$ (Fig. 7, dashed line), i.e. in this case an outer radius of 160 AU is found. However, as can be seen in Fig. 7, this model fails to explain the observed 60 μ flux. The breakdown of the simple model may be due to a change in the absorption efficiency of the dust grains at far-IR wavelengths (e.g. Jones and Merrill, 1976), which is not accounted for in our model.

We conclude that the observed excess in 51 Oph can be explained by an optically thin dust model with dust temperatures between about 1000 K and 120 K. The density distribution of the dust grains varies as r^{-m} with $m \simeq 1.3$, and the absorption efficiency of the grains $p \simeq 1$ to 2. The outer radius of the dust shell lies in the range $16{,}800 < x_1 < 2.7\,10^5$, depending on the value of p.

6. Discussion and conclusions

A remarkable property of the dust around 51 Oph is its wide temperature range, which allows the determination of the density distribution of the dust grains. We find $n(r) \propto r^{-m}$ with $m \simeq 1.3$, and in any case $m < 2$. A constant velocity outflow requires $m = 2$. This is excluded by the shape of the excess flux energy distribution. It thus seems likely that the dust grains are not part of a continuous outflow of a gas/dust mixture, but may be orbiting the star. The high rotational velocity ($v \sin i = 220$ km s^{-1}; Slettebak, 1982a) may indicate that the dust in 51 Oph is not distributed spherically symmetric, but may be concentrated in a disc, as is the case for β Pic (Smith and Terrile, 1984; Gillett, 1986). The size of the dust region for both stars is comparable (400 AU for β Pic). The dust temperatures found in β Pic range between 180 and 48 K (Gillett, 1986). The latter author concluded that the dust around β Pic cannot be radiating as blackbodies for $\lambda > 3.7\,\mu$, and that the IRAS far-IR energy distribution is consistent with $m = 1$ and $p = 1$, i.e. very close to the values found for 51 Oph. The fact that the dust around 51 Oph does not radiate as a blackbody indicates that the grain size is small compared to the wavelength of the observations. Particles of radius a radiate as blackbodies at wavelengths $\lambda \ll 2\pi a$. We observe deviations from blackbody emission at least at $\lambda > 60\,\mu$, implying grain sizes less than 9 μ. A lower limit to the size of the dust particles can be derived by considering the effect of radiation pressure on dust grains. For black grains, the "blow-out" radius for an A0 V star is estimated to be about 14 μ (Gillett, 1986). If the dust particles are not black, the blow-out radius may be larger, depending on the absorption and scattering properties of the grains. It is possible that in 51 Oph the formation of dust is still continuing, a fact which may be related to the Be nature of 51 Oph. The inner radius of the dust region is found at a temperature close to the maximum dust temperature possible for dust grains, suggesting that the inner radius is set by the UV radiation field of the Be star.

It is remarkable that dust formation mostly occurs in Ae and A-shell stars, and is almost absent in "classical" Be stars. Dust emission is observed in extreme Be stars, the B[e] or Bep stars, with spectral types as early as B2. These stars show low-excitation forbidden lines in the visual spectrum, which is usually interpreted in terms of very high densities in the circumstellar shell (for a review, see Underhill and Doazan, 1982). So apparently circumstellar dust can form either in very high-density material around the star (and in that case the spectral type of the primary is not important), or when the effective temperature of the star is lower than about 10^4 K.

There are a number of striking similarities between the properties of the circumstellar matter around 51 Oph and β Pic. For both stars it is likely that inside the dust shell there is ionized gas. For β Pic this can be inferred from the "shell star" classification (Slettebak, 1982a). Vidal-Madjar et al. (1986) derived a density distribution of the gas in the circumstellar disc of β Pic, and found $\rho(r) \propto r^{-n}$ with $0 \leq n \leq 1$, consistent with the density distribution of the dust grains (Gillett, 1986), and of the same order as the density distribution of the dust in 51 Oph. The presence of ionized material around 51 Oph can be inferred from the Be classification. Slettebak (1982a) notes that "Hβ has a sharp central absorption component with weak flanking emission". Such a line profile is indicative of a shell spectrum. Thus it may very well be that 51 Oph is seen close to equator-on. The major difference between 51 Oph and β Pic is the hot dust in 51 Oph, and the fact that 51 Oph is a Be star. The Be classification indicates that there is high-density *ionized* material around 51 Oph.

The similarities between 51 Oph and β Pic suggest a possible connection between both stars. Aside from the IR excess observed in β Pic, this star is a "typical" A-shell star (e.g., Slettebak, 1982a; Slettebak and Carpenter, 1983; Kondo and Bruhweiler, 1985; Hauck, 1987). The A and F type shell stars are thought to be the cool extension of the Oe/Be sequence (e.g., Slettebak, 1982b; 1986; Jaschek et al., 1987). The major difference between the Be and the A/F-shell stars is the absence of Hα emission in the latter group. The transition between (strong) Hα emission and Hα absorption occurs quite abruptly at spectral type A0 (Slettebak, 1986; Jaschek et al., 1987). Slettebak (1986) interprets this transition as due to the decrease in the effective temperature of the star. Given the fact that β Pic and 51 Oph are members of the Be/A-shell star group and given the many similarities between the circumstellar shells of both stars pointed out above, we

speculate that in both stars a similar mechanism may be responsible for the presence of the circumstellar material.

In recent literature it has been suggested that the disc of β Pic is a *proto-planetary disc*, similar to the ones observed in α Lyr, α PsA and ϵ Eri (Gillett, 1986; Smith and Terrile, 1984). However, there are a number of differences between β Pic and the other stars discussed by Gillett (1986), i.e. α Lyr, α PsA and ϵ Eri. The dust in β Pic is hotter than that around the other stars: there is already a considerable excess at 12 μ, while the other stars show no evidence for dust at that wavelength. Furthermore, the IR excess of α Lyr, α PsA and ϵ Eri can be fitted by "black" grains, suggesting the presence of very large grains, whereas for β Pic "black" grain models cannot explain both the temperature of the dust *and* the size of the dust region, indicating that the grains in the disc around β Pic are considerably smaller. The presence of circumstellar material in β Pic was already known from the visual and UV spectrum before the discovery of the large IR excess. For α Lyr and α PsA, no strong evidence for the presence of ionized circumstellar material can be found in the spectrum. However, this may be due to viewing angle effects.

From the above discussion it is clear that the nature of 51 Oph and β Pic is still poorly understood. If the disc observed around β Pic is a proto-planetary disc, i.e. a remnant of the cloud from which the star was formed, the question arises what the relation is between the A/F shell stars (of which β Pic is a member) and the stars with proto-planetary discs. It is possible that a shell star classification can result from two physically completely different types of objects, namely stars with proto-planetary discs and stars in which matter is ejected into an equatorial disc by a mechanism similar to the one effective in Be stars. If this is the case, it is not possible at present to decide whether a proto-planetary disc is present around 51 Oph. It is clear however that the detection of a large amount of dust in 51 Oph is not typical for Be stars.

Recently, Ferlet et al. (1987) suggest on the basis of observations of variable Ca II-K absorption in β Pic, that its disc is composite, with an inner part typical for shell stars, and a more extended one, unrelated to the inner one, containing the dust. They also suggest that this is unique to β Pic. However, the observations of 51 Oph presented in this paper show that the combined presence of gas and dust is not restricted to β Pic and may be more widespread. The question whether or not these two components are unrelated needs further attention.

We plan to continue the study of the properties of the circumstellar material around 51 Oph by means of IUE and high-resolution optical spectra. 51 Oph may also be a good candidate to search for evidence of the dust in the optical using the Faint Object Camera at ESO.

Acknowledgements. The authors gratefully acknowledge interesting discussions on this topic with H. Lamers, and also for suggesting the title of this paper. LBFMW acknowledges financial support from the Netherlands Organization for Pure Scientific Research ZWO. We thank the referee for constructive remarks.

References

Ashok, N.M., Bhatt, H.C., Kulkarni, P.V., Joshi, S.C.: 1984, *Monthly Notices Roy. Astron. Soc.* **211**, 471
Coté, J., Waters, L.B.F.M.: 1987, *Astron. Astrophys.* **176**, 93 (Paper I)
Dachs, J., Wamsteker, W.: 1982, *Astron. Astrophys.* **107**, 240
Explanatory Supplement to the IRAS Catalogues and Atlases, Eds. C.A. Beichman, G. Neugebauer, H.J. Habing, P.E. Clegg and T.J. Chester (1985)
Ferlet, R., Hobbs, L.M., Vidal-Madjar, A.: 1987, *Astron. Astrophys.* **185**, 267
FitzGerald, M.P.: 1971, *Astron. Astrophys.* **4**, 234
Gehrz, R.D., Hackwell, J.A., Jones, T.W.: 1974, *Astrophys. J.* **191**, 675
Gillett, F.: 1986, in *Light on Dark matter*, Ed. F.P. Israel, page 61
Hauck, B.: *Astron. Astrophys.* **177**, 193
Jaschek, M. Jaschek, C., Andrillat, Y.: 1987, (in press)
Jascheck, M., Jascheck, J., Egret, D.: 1986, *Astron. Astrophys.* **158**, 325
Johnson, H.L., Mitchell, R.I., Iriarte, B., Wisniewski, W.Z.: 1966, Comm. of the Lunar and Planetary Laboratory no. 63, Vol. 4, part 3
Jones, T.W., Merrill, K.M.: 1976, *Astrophys. J.* **209**, 509
Kondo, Y., Bruhweiler, F.C.: 1985, **291**, Ll
Kurucz, R.L.: 1979, *Astrophys. J. Suppl.* **40**, 1
Mezger, P.G., Mathis, J.S., Panagia, N.: 1982, *Astron. Astrophys.* **105**, 372
Poeckert, R., Marlborough, J.M.: 1978, *Astrophys. J. Suppl.* **38**, 229
Savage, B.D., Mathis, J.S.: 1979, *Ann. Rev. Astron. Astrophys.* **17**, 84
Slettebak, A.: 1982a, *Astrophys. J. Suppl.* **50**, 55
Slettebak, A.: 1982b, in *Be stars* IAU symp. no. 98, eds. M. Jaschek and H. Groth, page 109
Slettebak, A.: 1986, *Publ. Astron. Soc. Pacific* **98**, 867
Slettebak, A., Carpenter, K.G.: 1983, *Astrophys. J. Suppl.* **53**, 869
Smith, B.A., Terrile, R.J.: 1984, *Science* **226**, 1421
Sopka, R.J., Hildebrand, R., Jaffe, D.T., Gatley, I., Roellig, T., Werner, M., Jura, M., Zuckerman, B.: 1985, *Astrophys. J.* **294**, 242
Thompson, G.I., Nandy, K., Jamar, C., Monfils, A., Houziaux, L., Carnochan, D.J., Wilson, R.: 1978, "Catalogue of Stellar Ultraviolet Fluxes", ESA SR-28
Underhill, B.A., Doazan, V.: 1982, "B stars with and without emission lines" NASA SP-456
Vidal-Madjar, A., Hobbs, L.M., Ferlet, R., Gry, C., Albert, C.E.: 1986, *Astron. Astrophys.* **167**, 325
Waters, L.B.F.M., Coté, J., Lamers, H.J.G.L.M.: 1987, *Astron. Astrophys.* **185**, 206
Wright, A.E., Barlow, M.J.: 1975, *Monthly Notices Roy. Astron.* Soc. **178**, 41